IOP Conference Series: Materials Science and Engineering

PAPER • **OPEN ACCESS**

PIV Experimental Study of the Axial Flow Blood Pump's Internal Flow Field Under Pulsatile Condition

To cite this article: Shuai Wang *et al* 2018 *IOP Conf. Ser.: Mater. Sci. Eng.* **423** 012104

IOP Conf. Series: Materials Science and Engineering **423** (2018) 012104 doi:10.1088/1757-899X/423/1/012104

PIV Experimental Study of the Axial Flow Blood Pump's Internal Flow Field Under Pulsatile Condition

Wang Shuai, Tan Jianping, Yu Zheqin, Xiao Zhiyong, Wu Weiqiang, Cheng lizhi

School of Mechanical and Electrical Engineering, Central South University, Changsha 410083, China

E-mail: jptan@163.com

Abstract. Taking the axial flow blood pump as the research object, we used the particle image velocimetry (PIV) to measure the flow distribution of inlet, outlet and impeller at the changing rotation speed. Effects of the acceleration and deceleration process on the change of internal flow field were compared and analyzed. The experimental results show that the flow field of inlet and outlet area of the blood pump is stable at the constant working speed, but the vortex and reflux exist in the impeller area. However, acceleration of the impeller increases the flow field's volocity and disturbance. Deceleration of the impeller rotation speed reduces the flow velocity, and the flow state of overall flow field is relatively stable. Design of the pulsatile blood pump should be optimized in order to reduce the occurrence of hemolysis in the process of acceleration and deceleration.

1. Introduction

At present, there are more than twenty million of the heart failure patients worldwide[1], and it is now rising rapidly because of the aging of the population[2]. The treatment of heart support through the implantation of blood pump artificial heart has become the best treatment for the lack of heart donor. The widely used blood pump is the second generation and the third generation blood pump. Which working principle is to generate continuous output flow by rotating the impeller. However, commercially blood pumps use constant speed mode to provide continuous flow for the body generally. With long-term continuous flow assisted, the human body can lead to impaired renal function [3-4], ischemic and hemorrhagic stroke [5], vascular dysfunction[6], oxidative stress [7], and the digestive tract arteriovenous malformation[8] and aortic stiffness increased[9]. These adverse effects have become one of the key problems that restrict the development of blood pumps.

Based on the above problems, experts have proposed that the pulsation flow similar to the heart can be generated by rapid and periodic changes in the speed of the blood pump, which causes the blood pump to work at the non-design point, and the internal flow field will change violently, which will affect the hemolysis performance of the blood pump. Therefore, it is necessary to study the internal flow field of the blood pump under pulsating condition, and analyze the effect of the variable speed on the flow field.

Chen Z [10] used CFD simulation to analyze the transient state of the axial flow pump and centrifugal pump under the pulsating flow condition, and pointed out that the high hemolysis area may appear in the interior of the pump. F Shu [11] used PIV to shoot the flow field of the centrifugal blood pump in the pulsating mode, and analyzed the time-varying characteristics of the internal flow field. Wong, K, C and other [12] used PIV to rotate the blood pump in the pulsating condition of 5 different geometric shapes at the outlet of the flow field.

IOP Conf. Series: Materials Science and Engineering **423** (2018) 012104 doi:10.1088/1757-899X/423/1/012104

2. Experimental model

The experimental model was designed by the axial blood pump designed by Central South University. As shown in Figure 1, it contained pre-turning vane, impeller and rear guide vane. The impeller contained permanent magnets, which can drive the impeller of the blood pump to rotate through an external magnetic field. The design flow is 5L/min, pressure difference is 13.3Kpa, speed is 8000r/min, and material is titanium alloy. In order to reduce the anti-light in the PIV experiment, the parts of the blood pump was processed in black.

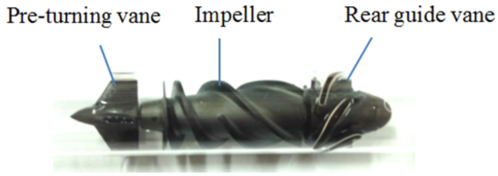

Figure 1. experimental blood pump model

3. Experimental device

3.1. PIV experimental system

The PIV experimental device adopted the LaVision PIV system (German). The main components are as follows: The laser is Litron LDY300 with the highest working frequency of 90Hz, and the PIV camera is a LaVision ImagerProSX 5M double shutter camera with a resolution of 2448x2050. The synchronous shooting system includes 1108090 synchronizer, rotation Encoder, signal transmission cable and Davis processing software.

3.2. Layout of Test-bed

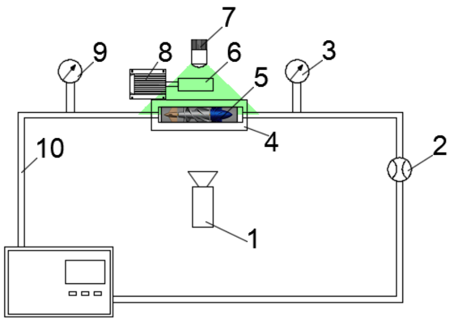

Figure 2. Layout of the test-bed

1. Camera 2. Flow Meter 3. Pressure Gauge 4. Refractive index matching water tank 5. Blood pump 6. Magnet 7. Laser head 8. Motor 9. Pressure gauge 10. Pipe 11. Thermostat water bath cauldron

The overall layout of the test-bed is shown in Figure 2, the blood pump was installed in a transparent acrylic circular pipe, a square index matching water tank was added to the outside side of the blood pump to reduce refraction. The laser was irradiated from the upper side of the blood pump and the camera was photographed in the direction perpendicular to the laser irradiation direction. In order to eliminate the occlusion of the driving device, a motor with strong magnets was arranged in the rear of the blood pump. The motor drived strong magnets to produce alternating magnetic fields to drive the blood pump, the rotation period of the external motor was two times of the blood pump. Furthermore, the external motor was installed with a rotary encoder to output the shooting trigger Signal.

4. Experimental measurement method

4.1. Selection of fluid and tracer particle

In order to simulate the fluid properties of blood, 27.3% glycerol solution with a density of 1.07kg/m3 was chosen. In order to ensure good particle following and light scattering, the 10 μ m hollow glass beads were used to simulate the movement of blood cells in the flow field.

4.2. Shooting scheme

The inlet, impeller and outlet area were selected respectively for shooting. The speed regulation waveform of the blood pump is shown in Figure3. At the beginning, the 0s~0.5s and 1.5s~2s are taken as the stable stage, and the 0.5s~1.5s is the variable speed stage.

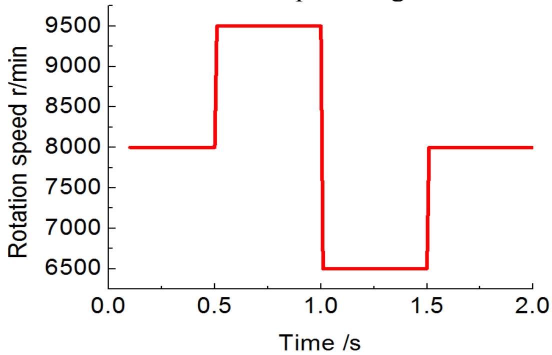

Figure 3. Rotation speed control curve of blood pump

4.3. PIV software setup

The time interval of the inlet, outlet and impeller area of the blood pump was set 150 μ s, 150 μ s and 50 μ s respectively. In the Davis software, the camera shooting mode was selected as the external trigger mode, the frequency of the shooting was the same as the output signal frequency of the external motor encoder, and the blood pump was taken once every two cycles. The size of the inquiry window was set to 32×32, and the adaptive PIV algorithm was chosen.

5. Experimental results and analysis

The experimental results show the absolute velocity of the flow field, in which the arrow indicates the direction of speed and the color is the size of the velocity. Due to the large number of pictures, 2 pictures are selected for analysis in the stages of steady speed (8000r/min), acceleration (8000r/min~9500r/min), deceleration (9500r/min~6500r/min) and acceleration to steady speed(6500r/min~8000r/min).

5.1. Flow field distribution of the inlet area

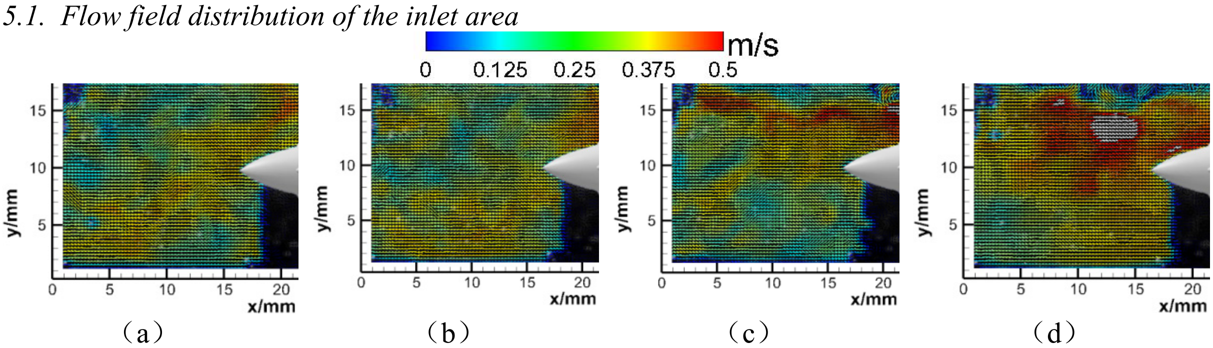

IOP Conf. Series: Materials Science and Engineering **423** (2018) 012104 doi:10.1088/1757-899X/423/1/012104

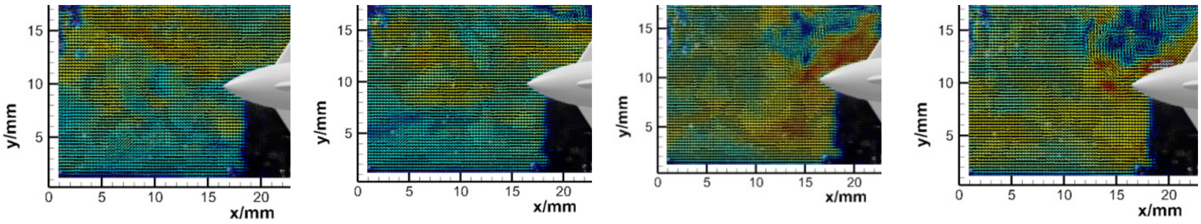

（e） （f） （g） （h）

Figure 4. Flow field distribution of the inlet area

(a) (b) 8000r/min (c) (d) 8000~9500r/min (e) (f) 9500~6500r/min (g) (h) 6500~8000r/min

According to figure 4, the velocity distribution of the inlet is stable at the steady speed. The particles’ velocity direction in the flow field is basically the same as the axis direction. The velocity direction of the flow field near the pre-turning vane is consistent with the vane’s shape. At the rotational speed of 8000~9500r/min, the velocity of the inlet flow field has obviously increased, unstable flow has been generated in the flow field, a clear vortex is produced in the upper right corner of Figure 4 (c), there is a serious flow separation in the upper wall of the near pipeline in Figure 4 (d), so the acceleration of the impeller will have a certain effect on the inlet, and the flow field is disorganized. In the process of 9500~6500r/min, the velocity of the flow field is reduced and the vortex appears in the upper right. At 6500~8000r/min, the flow field has a large area of vortex distribution and flow separation in the upper right.

5.2. Flow field distribution of the impeller area

As shown in Figure 5 (a), the impeller flow field area is divided into four regions: A, B, C, D according to the separation of blades.

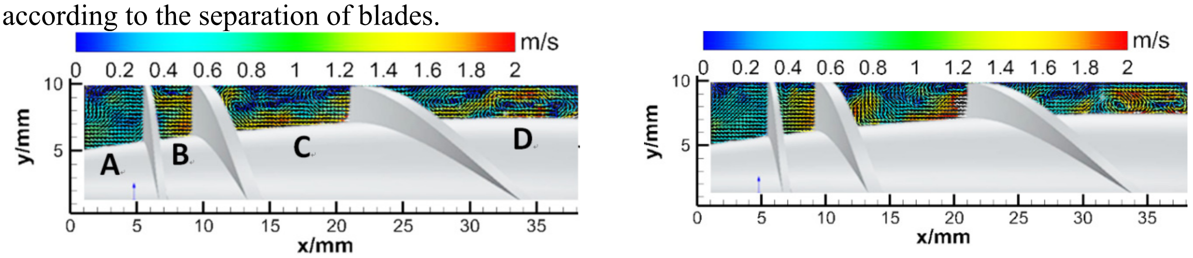

（a） （b）

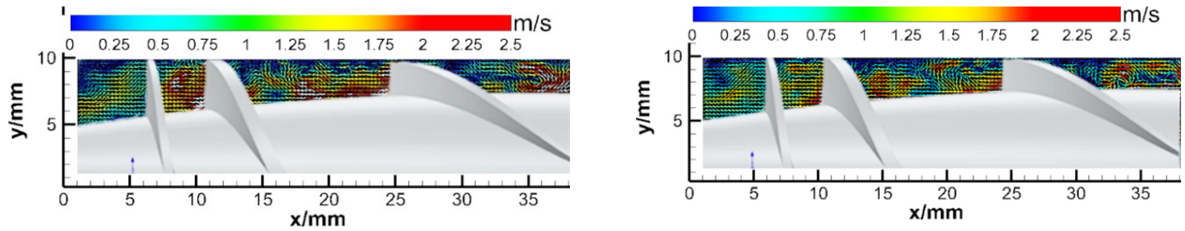

（c） （d）

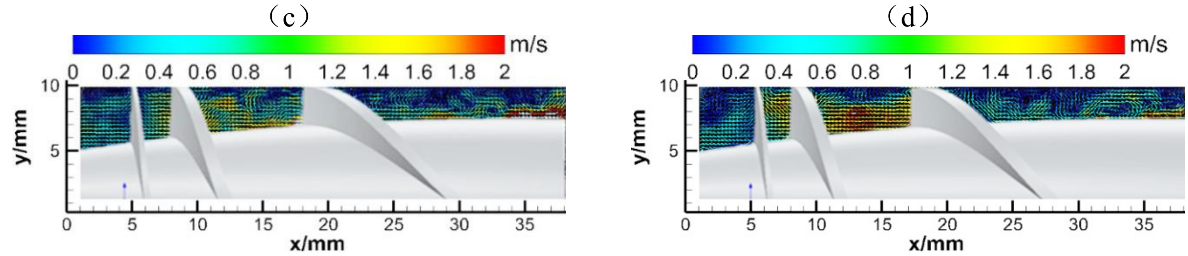

（e） （f）

IOP Conf. Series: Materials Science and Engineering **423** (2018) 012104 doi:10.1088/1757-899X/423/1/012104

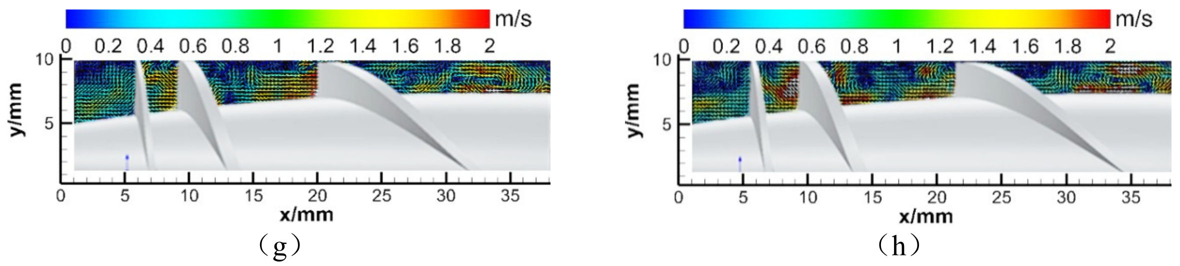

Figure 5. Flow field distribution of the impeller area

(a) (b) 8000r/min (c)(d) 8000~9500r/min (e)(f) 9500~6500r/min (g)(h) 6500~8000r/min

As shown in Figure 5, the velocity of A, B and C increases in turn at the stable speed of 8000r/min. The distribution of the flow field in the A, B and C region is more stable. Due to the hindrance effect of the rear guide vane, the velocity of D region decreases, and the unstable flow state such as reflux and vortex appear. Compared with the stable state, in the process of 8000~9500r/min, the velocity of the C region near the hub increases, the phenomenon of flow separation increases. The reflux still exists in the D region, the velocity of the flow field increases with the increase of the speed. In the process of 9500~6500r/min, the flow field of A, B and C is basically stable and the velocity direction is parallel to the axis. The velocity of the flow field in the D region is smaller, but there is a backflow phenomenon at the outlet and the number of the vortices increases. In the process of 6500~8000r/min, the distribution of flow field is similar to the 8000~9500r/min stage, the flow field is disturbed in the C region, there is a phenomenon of reflux and flow separation at the outlet of the D region.

5.3. Flow field distribution of the outlet area

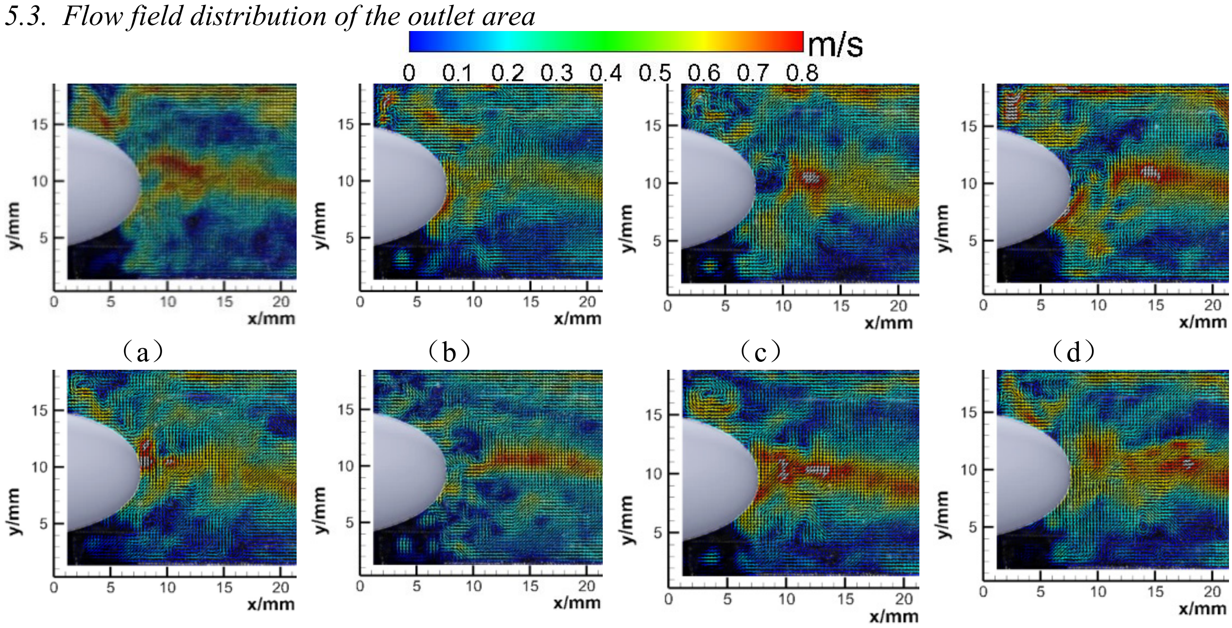

Figure 6. Flow field distribution of the outlet area

(a) (b) 8000r/min (c) (d) 8000~9500r/min (e)(f) 9500~6500r/min (g) (h) 6500~8000r/min

As shown in Figure 6, at the stable speed of 8000r/min, the streamline at the edge of the rear guide vane is basically consistent with the outline of the rear guide vane, and a high speed belt appears at the upper wall and center of the outlet area. In the process of 8000~9500r/min, speed of the flow center increases, the flow separation and vortex appear at the top wall of the rear guide vane, the number of vortices in the flow field increases, also the disturbance of the flow field increases. During the deceleration process of 9500~6500r/min, the overall velocity in the flow field decreases, and the flow around the rear guide vane is basically the same as the external contour. In the process of

6500~8000r/min, the overall velocity distribution increases, but a larger vortex appears above the rear guide vane.

6. Conclusion

(1) At the stable speed, the flow field in the inlet area of the blood pump is stable, but the vortex and reflux exist in the region of the outlet of the impeller, which is caused by the obstruction of the rear guide blade.

(2) During the acceleration of blood pump, vortex appears above the leading edge of the blood pump. The D region of impeller shows obvious separation of flow, increase of vortex number and reflux velocity. The phenomenon of flow separation and vortex also appears in the outlet area. The main reason is that the acceleration of impeller is large and the Reynolds number of the flow field increases rapidly. Therefore, the unstable flow state of the flow is aggravated.

(3) In the process of deceleration, the velocity of the inlet, impeller and outlet decreases, the overall flow state is more stable than the accelerated process, but vortexes exist at the outlet of the impeller area.

(4) In the process of variable speed, the Reynolds number inside the flow field changes rapidly, the disturbance of the internal flow field increases obviously in the process of acceleration, which will inevitably have a bad effect on the hemolytic performance of the blood pump. Therefore, the structure of blood pump should be optimized according to the flow field distribution in the speed change process, so as to reduce the production of hemolysis during the process of the speed change.

Acknowledgments
This work was supported by National Natural Science Foundation of China (Grant No. 51475477, 31670999).

References

[1] Bui, A. L., Horwich, T. B., & Fonarow, G. C. (2011). Epidemiology and risk profile of heart failure. Nature Reviews Cardiology, 8(1), 30-41.
[2] Smolina, K., Wright, F. L., Rayner, M., & Goldacre, M. J. (2012). Determinants of the decline in mortality from acute myocardial infarction in england between 2002 and 2010: linked national database study. Bmj, 344(jan25 2), d8059.
[3] Borgi, J., Tsiouris, A., Hodari, A., Cogan, C. M., Paone, G., & Morgan, J. A. (2013). Significance of postoperative acute renal failure after continuous-flow left ventricular assist device implantation. Annals of Thoracic Surgery, 95(1), 163.
[4] Patel, A. M., Adeseun, G. A., Ahmed, I., Mitter, N., Rame, J. E., & Rudnick, M. R. (2013). Renal failure in patients with left ventricular assist devices. Clinical Journal of the American Society of Nephrology Cjasn, 8(3), 484.
[5] Starling RC; Moazami N; Silvestry SC; Ewald G; Rogers JG; Milano CA; Rame JE; Acker MA; Blackstone EH; Ehrlinger J; Thuita L; Mountis MM; Soltesz EG; Lytle BW; Smedira NG. (2014). Increase in left ventricular assist device thrombosis. New England Journal of Medicine, 370(1), 33-40.
[6] Gambillara, V., Thacher, T., Silacci, P., & Stergiopulos, N. (2008). Effects of reduced cyclic stretch on vascular smooth muscle cell function of pig carotids perfused ex vivo. Journal of Biomechanics, 39(4), S279-S279.
[7] Thacher, T., Gambillara, V., Da, S. R., Silacci, P., & Stergiopulos, N. (2010). Reduced cyclic stretch, endothelial dysfunction, and oxidative stress: an ex vivo model. Cardiovascular Pathology, 19(4), e91-e98.
[8] Demirozu, Z. T., Radovancevic, R., Hochman, L. F., Gregoric, I. D., Letsou, G. V., & Kar, B., et al. (2011). Arteriovenous malformation and gastrointestinal bleeding in patients with the heartmate ii left ventricular assist device. Journal of Heart & Lung Transplantation the Official Publication of the International Society for Heart Transplantation, 30(8), 849-853.

[9] Nassif, M. E., Tibrewala, A., Raymer, D. S., Andruska, A., Novak, E., & Vader, J. M., et al. (2015). Systolic blood pressure on discharge after left ventricular assist device insertion is associated with subsequent stroke. Journal of Heart & Lung Transplantation, 34(4), 503-508.

[10] Chen, Z., Jena, S. K., Giridharan, G. A., Koenig, S. C., Slaughter, M. S., & Griffith, B. P., et al. (2017). Flow features and device-induced blood trauma in cf-vads under a pulsatile blood flow condition: a cfd comparative study. International Journal for Numerical Methods in Biomedical Engineering, 34(2), e2924.

[11] Shu, F., Vandenberghe, S., Brackett, J., & Antaki, J. F. (2015). Classification of unsteady flow patterns in a rotodynamic blood pump: introduction of non-dimensional regime map. Cardiovascular Engineering & Technology, 6(3), 230-241.

[12] Wong, K. C., Büsen, M., Benzinger, C., Gäng, R., Bezema, M., & Greatrex, N., et al. (2014). Effect of rotary blood pump pulsatility on potential parameters of blood compatibility and thrombosis in inflow cannula tips. International Journal of Artificial Organs, 37(12), 875-87.